Results in Optics 21 (2025) 100861

Contents lists available at ScienceDirect

Results in Optics

journal homepage: www.elsevier.com/locate/rio

Invited article

Experimental determination of Arrhenius degradation coefficients for monocrystalline photovoltaic solar cells

Rui G. Marques Araújo [a], Ricardo A. Marques Lameirinhas [b,*], João Filipe Pereira Fernandes [a,c], Rui J. Tomás Oliveira [a], Catarina P. Correia V. Bernardo [a,b], João Paulo N. Torres [b,d]

[a] Instituto Superior Técnico - Universidade de Lisboa, Av. Rovisco Pais, 1049-001, Lisboa, Portugal
[b] Instituto de Telecomunicações, Av. Rovisco Pais, Torre Norte, 10, 1049-001, Lisboa, Portugal
[c] IDMEC, Instituto Superior Técnico, Universidade de Lisboa, Av. Rovisco Pais, 1049-001, Lisboa, Portugal
[d] Academia Militar, Av. Conde Castro Guimarães, Amadora, 2720-113, Lisboa, Portugal

ARTICLE INFO

Keywords:
Accelerated ageing tests
Arrhenius model
Photovoltaic solar cell ageing
Ageing effects
Photovoltaic cells modelling
Degradation coefficients

ABSTRACT

As photovoltaic solar technology plays a pivotal role in the transition to renewable energy, concerns about long-term performance still persist. This research aims to investigate and model the ageing effects in photovoltaic solar cells, defining power and voltage degradation coefficients. Monocrystalline modules from two different manufactures are tested. The objective is to provide quantitative insights into performance decline over time, offering guidance for improving photovoltaic system reliability. Photovoltaic solar cells are subjected to accelerated ageing tests considering high temperature conditions to increase electron collisions, emulating long-term operation. It is verified that open-circuit and maximum power point present a logarithm decline trend over time. On the other hand, the accelerated temperature ageing tests allow us to apply the Arrhenius model, which also represents logarithm behaviour but with the temperature. This is used to predict real-world degradation trends. Results showed that maximum power output declines between 0.22% and 0.80% per year, depending on the manufacturer. Moreover, the V_{oc} presents a faster degradation rate, decreasing 10% in approximately 4 years. The model results present high coefficients of determination, confirming the strong correlation between empirical data and theoretical models.

1. Introduction

In an era marked by the urgent need for sustainable and renewable energy sources, photovoltaic (PV) solar energy has become a consolidated alternative in the fight against climate change and the depletion of fossil fuels. The adoption of PV solar systems has witnessed unprecedented growth worldwide, with solar energy installations proliferating at an exponential rate. PV technology is easy to install and maintain and is not expensive compared with other renewable sources, mainly because the most used materials are abundant in the Earth and the fabrication processes are well-known.

As PV system age, they gradually lose some performance. Most commonly, PV module manufacturers guarantee a maximum loss of about 20% of power after 25 years. The decline is expressed in relative percentage, such that a module with a hypothetical absolute efficiency of 20% today would decline to 17.5% after 25 years at a rate of 0.5%/year, assuming a linear decline (Jordan et al., 2016; Jordan and Kurtz, 2013; Gebhardt et al., 2025).

Generally, solar panels have a warranty of 25–30 years. Knowing that the usual return on investment of a photovoltaic system can be up to 10 years, this means that, after the initial investment is recovered, the solar panels can output between 10% to 20% less than their original production output. Typically, a 20% decline is considered a failure, but there is no consensus on the definition of failure. The identification of the underlying degradation mechanism through experiments and modelling can lead directly to lifetime improvements (Jordan and Kurtz, 2013).

This work provides experimental and quantitative results on the changes of the electrical response in the PV solar cells due to their ageing. To accomplish so, a methodology based on accelerated ageing techniques is presented, allowing one to reproduce the effect of dozens of years under normal operation into hundreds of hours under accelerated conditions. In the end, these quantitative results will allow the modelling of this type of phenomenon in the characteristics of the solar cells.

* Corresponding author.
E-mail address: ricardo.lameirinhas@lx.it.pt (R.A. Marques Lameirinhas).

https://doi.org/10.1016/j.rio.2025.100861
Received 21 May 2025; Received in revised form 18 June 2025; Accepted 21 June 2025
Available online 4 July 2025

2. Literature review on solar cells ageing phenomena

The ability to accurately predict power delivery over time is of vital importance to the growth of the PV industry. Two key cost drivers are the efficiency with which sunlight is converted into power and how this relationship changes over time. An accurate quantification of power decline over time, also known as degradation rate, is essential to all stakeholders. Financially, the degradation of a PV module or system is equally important, because a higher degradation rate translates directly into less power produced and, therefore, reduces future cash flows, as well as indirectly to new investment to substitute modules (Jordan and Kurtz, 2013).

With the emergence of different technologies of PV cells it becomes imperative to access each technology ageing. Their characteristics must be studied since they will influence the behaviour of the PV solar cells with ageing. In this section, a brief explanation of each type of PV solar cell as well as previous developed research on their ageing will be presented.

Of all the technologies of PV cells, wafer-based silicon account for 90% of the PV solar cells. The most manufactured solar cells are monocrystalline, polycrystalline a-Si, CdTe and CIGS. Based on manufacturing material and level of commercial maturity, PV cell technologies can be categorised into three generations (Rathore et al., 2021).

2.1. First generation PV solar cells — Silicon wafers

Crystalline silicon PV solar cells have been present for quite some time. And even with the development of several alternatives to silicon-based PV cells, it remains as the most widespread and prevalent PV technology today, accounting for 95% of produced photovoltaic solar power in 2020 (Marques Lameirinhas et al., 2022). In the first generation, there are two types of silicon PV solar cells: monocrystalline and polycrystalline.

These cells reveal a substantial decrease of its efficiency, with reported median degradation rate of 0.5–0.6%/year and a mean in the 0.8 – 0.9%/year range (Jordan et al., 2016; Gebhardt et al., 2025; Libby et al., 2023).

One of the main deterioration aspects is a considerable deterioration of the optical properties of the tempered glass and of the Ethylene Vinyl Acetate (EVA) encapsulate, which is the main responsible for the efficiency rundown to around 86.5% of its initial value after a lifetime of 25 years in Standard Test Conditions (STC). Besides that, the EVA encapsulate does not tolerate temperatures above 100 °C, which conditions high-temperature experimental tests made on PV solar cells. Indeed, the alteration of the electrical properties of materials (p–n junction and electrodes) represents only 13.5% of this diminution. The degradation rate of the maximum power for a monocrystalline was reported to be 0.5%/year (Doumane et al., 2015a; Libby et al., 2023).

2.2. Second generation PV solar cells — Thin films

This generation is based on thin-film PV technologies, where three main families are included: amorphous silicon (a-Si) and micromorph silicon (a-Si/μc-Si), cadmium telluride (CdTe) and copper indium gallium selenide (CIGS). Second-generation cells were developed with the intent of reducing the costs of the previous generation and improving their characteristics (Marques Lameirinhas et al., 2022). However, they offer a slightly lower efficiency, and some technologies use highly toxic metals (such as Cadmium, which is specifically listed in the European Restriction of Hazardous Substances Directive — RoHS) or rare (as Indium) (Mughal et al., 2018). Maybe due to that, accelerated tests in CIGS are not common in literature.

Amorphous silicon (a-Si) is the most commonly developed and non-crystalline allotropic form of silicon. It is most popular among thin film technology, but it is prone to degradation (Gul et al., 2016). Besides that, this technology is also less efficient than crystalline silicon, with typical efficiencies of around 6%, but it tends to be easier and cheaper to produce (Mughal et al., 2018). Several studies have been done to analyse how a-Si PV solar cells age. In King et al. (2000), results show that only after 6 months, this type of cells already show some degradation. Besides that, the majority of the analysed modules reach a stabilised power level about 20% below the initial power after about 1 year (King et al., 2000).

CIGS solar cell comprises four elements, i.e., copper, indium, gallium, and selenium. It has achieved efficiencies of 20% (Ott et al., 2013). However, they are expensive and usually difficult to obtain in the market, not only due to the fabrication processes but also due to the indium rarity in the Earth (Rathore et al., 2021). In Ott et al. (2013) the authors tested some cells of this technology, verifying that the degradation rate of the open-circuit voltage ensures 35 years of performance.

From an economical point of view, CdTe is one of the most important types among thin-film PV solar cells which is less expensive and economically feasible as well. The p–n junction diode is formed between layers of cadmium sulphide (Rathore et al., 2021). In this type of cell, the degradation appears to result from a decrease in the carrier concentration with ageing. The authors in Tyan (1988) reported a decrease between 6% to 10% after about 2 years of operation.

2.3. Third generation PV solar cells

Limitations seen in other PV technologies are lessened by the introduction of nanoscale components due to their enhanced optical properties, dielectric properties, heat resistance and mechanical properties such as stiffness, strength and resistance to wear and damage. Therefore, to improve conversion efficiency, nanoscale structures that absorb more solar radiation are favoured, not just those based on p–n junctions (El Chaar et al., 2011).

Due to their materials and fabrication processes, the technologies in this generation cannot be exposed to high temperatures, limiting accelerated tests. Furthermore, due to commercial and laboratory reproducibility, the most analysed technologies are perovskite solar cells, which also converge to today's application needs.

Perovskite PV solar cells are a newly developed PV solar cell type which has several advantages compared with thin-film PV solar cells and conventional silicon, such as higher efficiency, low-temperature solution processability, high absorption coefficient, long carrier-diffusion length, and tunable direct bandgap (Rathore et al., 2021; Marques Lameirinhas et al., 2022; Shin and Shin, 2023).

The first reported stable perovskite PV solar cells had conversion efficiencies as high as 9.7%, but today some solar cells have an overall efficiency up to 31%. Stability and durability are certain issues regarding perovskite type PV solar cells. Due to the degradation of the material used in this cell, the efficiency gets reduced at least two to three times faster than other technologies (Rathore et al., 2021; Zhou et al., 2023).

3. Methodology

3.1. Photovoltaic solar cells characterisation

PV solar cells are commonly modelled by one-diode equivalent circuits, namely 1M5P model since it considers losses. However, the I–V characteristics of this model do not fit well with the behaviour of some PV solar cells as well as under or after being under extreme conditions. The d1MxP is based on the discretisation of the diode's electrical behaviour. It does not use fitting processes, it is based on connecting adjacent experimental points (Torres et al., 2023a,b; Bernardo et al., 2024). While the information given by the d1MxP model regarding losses is yet to be direct as the ones given by the shunt and series resistance in 1M5P, it is able to provide a better characterisation of the points near the maximum power point and open circuit voltage, which is the main focus in this kind of works. This is essential because the conventional model always produces some inaccuracies due to the required fitting. These would be critical to evaluate the change of the maximum power point and open-circuit voltage along the ageing process. Therefore, the d1MxP is more adequate for this study. Thus, in this research work d1MxP model is used to consider the maximum power point, the open-circuit voltage and the short-circuit current experimentally obtained.

The discretisation is done using the diode's equivalent circuit, consisting of an ideal diode, resistance, and an independent voltage source in series. The diode is discretised in N branches, meaning that the electrical behaviour of the PV solar cell is linearised at each experimental I-V point (Torres et al., 2023a,b; Bernardo et al., 2024). This is especially important for points close to the point of maximum power. This approach allows the computation of more accurate I–V and P–V curves since the discrete model uses a larger portion of experimental points to describe the devices compared to the classical models presented in the literature that use a small portion of the data set to characterise the entire voltage range (Torres et al., 2023a,b; Bernardo et al., 2024; Adak et al., 2023). Also, if the point is experimentally measured, it may be in the model. Common fitting-based models cannot afford it.

3.2. Arrhenius model

The Arrhenius model is a commonly used method for forecasting the lifetime of electronic devices. The theory behind the Arrhenius model is based on the electron collision theory. Electronic devices age over time due to electron collisions. By increasing the temperature, electrons velocity is increased and consequently, collisions probability increases too. Thus, one can emulate ageing processes by increasing temperature and extrapolating results for normal conditions (van Leest et al., 2017; Sinha et al., 2020).

The relation between degradation rate (s^{-1}) and temperature, T, is shown in expression (1), where E_a denotes the activation energy, k the Boltzmann constant and A the parameter to fit the model for high temperatures (van Leest et al., 2017; Sinha et al., 2020). Instead of rate, the expression may be treated to determine the expected lifetime of electronic devices, as presented in expression (2). To simplify the extrapolation process and the extraction of physical meaning from data plots, Arrhenius graphics are commonly presented as shown in Eq. (3), resulted from the application of natural logarithms in both equation sides.

$$\upsilon \approx Ae^{(\frac{-E_a}{kT})} \tag{1}$$

$$t = Ae^{(\frac{E_a}{kT})} \tag{2}$$

$$ln(t) = \frac{E_a}{k}\frac{1}{T} + ln(A) \tag{3}$$

On the other hand, by increasing the temperature from the operation, T_{op}, to a certain value, T_{acc}, used to accelerate ageing, the Ageing Factor (AF) must be set according to expression (4) (van Leest et al., 2017; Sinha et al., 2020).

$$AF = \frac{(t_{op}) - (t_{op_0})}{(t_{acc}) - (t_{acc_0})} = A_{AF} \cdot e^{+B_{AF}(\frac{1}{T_{acc}} - \frac{1}{T_{op}})} \tag{4}$$

Based on this, electronic characteristics have an exponential age behaviour. Thus, the increase in temperature distorts the time scale. 1000 h in an oven at 80 °C can correspond to 20 years in an oven at 25 °C (i.e. normal conditions) (Barbato et al., 2017). This extrapolation starts by searching for the best A and B values to fit expression (3) at experimental data obtained for different T_{acc}. After that, T is set at 45 °C (nominal operating cell temperature) and one obtains the time t for which the degradation rate is equal to the obtained at high temperatures (the ones used for the accelerating ageing tests).

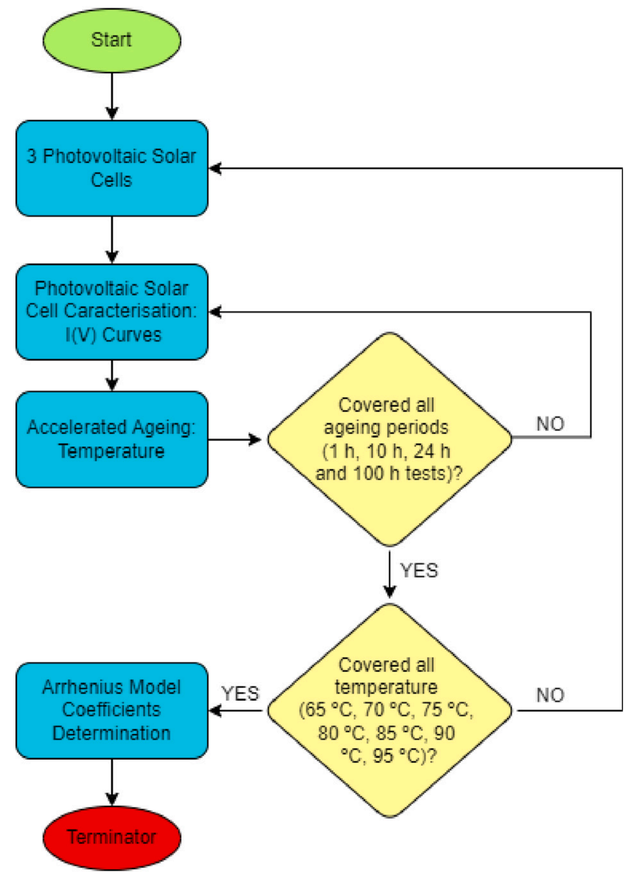

Fig. 1. Methodology flowchart.

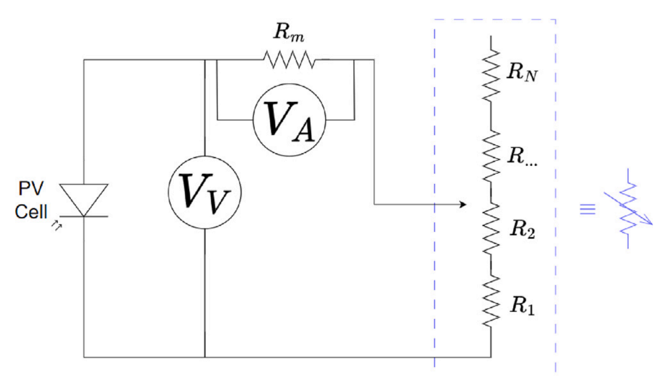

Fig. 2. Experimental set-up to obtain I–V points.

3.3. Experimental methodology

Firstly, a preliminary characterisation of the solar cell at 25 °C is done. After that, the cell is taken to the oven for 1 h at high temperature. After 1 h, the I-V characteristic of the cell is obtained after the cell reaches room temperature. This scheme is repeated for different accelerated ageing periods (1 h, 10 h, 24 h and 100 h tests — 135 h in total) and temperatures (65 °C, 70 °C, 75 °C, 80 °C, 85 °C, 90 °C, 95 °C). The methodology is summarised in the flowchart shown in the Fig. 1. The goal is to determine the coefficient A and the slope E_a/k of expression (3). As illustrated in the flowchart of Fig. 1, this is done after the experimental accelerating ageing procedures different temperatures and periods.

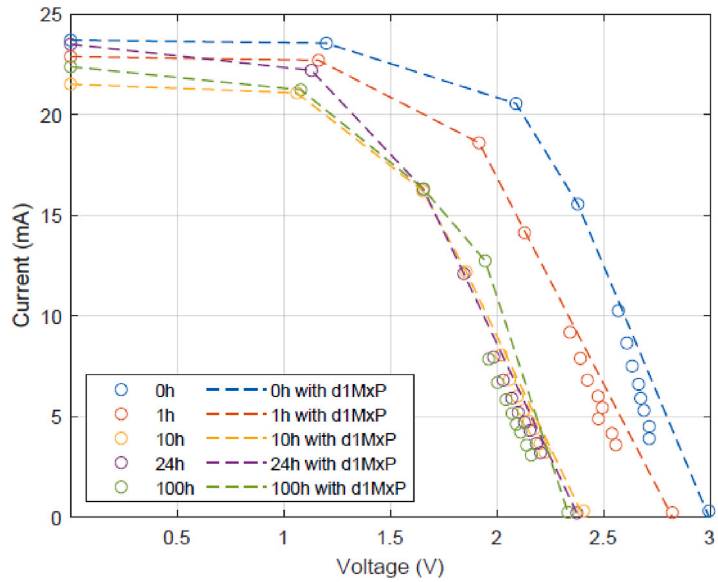

Fig. 3. Current–voltage curves of OSEPP SC10036 modules for 95 °C.

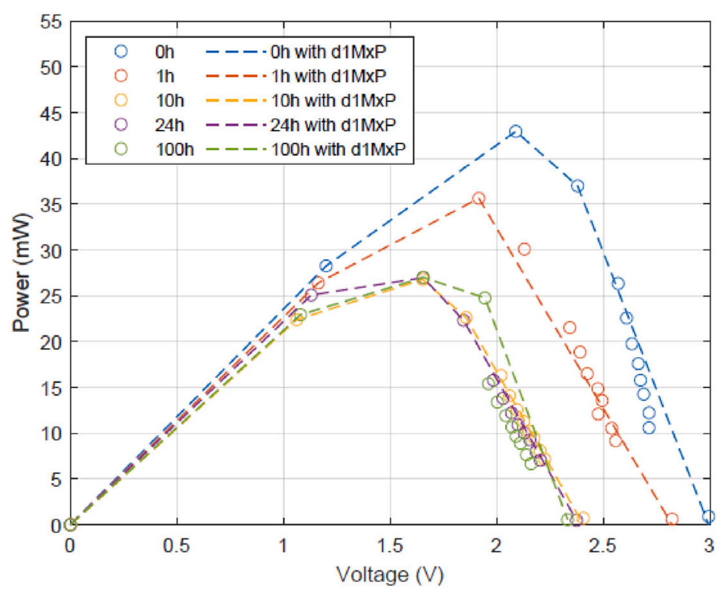

Fig. 4. Power-voltage curves of OSEPP SC10036 modules for 95 °C.

The accelerated ageing temperature tests are conducted by controlling only the temperature. The experimental current and the voltage are measured using GW Instek GDM-8135 multimeters both in DC Voltage mode. As illustrated in Fig. 2, a multimeter is measuring directly the voltage of the photovoltaic solar cell, V_V. Another one is used to measure the voltage in a measurement resistance R_m. This is a precision 10 mΩ resistance that allows us to reduce the load effect of a common ammeter.

The I-V points are obtained one by one, reducing noise and ensuring the same load conditions for each resistance for different tests.

To ensure the repeatability of the tests and the validation of the model that is created from the tests results, all the tests are conducted using 3 identical PV solar cells, using a 50 W light with a light temperature of 6400 K, under 84 W/m^2.

This strategy allows us to follow the evolution of the cell characteristics as I_{sc}, V_{oc} and P_{max}. With these values, I-V curves are plotted and the algorithm from the d1MxP model is used to connect experimental points.

Using I-V curves, the evolution of the aforementioned characteristics is traced in terms of time and experiment temperature.

4. Results

Based on the modules' efficiencies and today's market shares, we selected the monocrystalline solar cells to carry out the experimental tests. Two modules from two manufacturers are compared: (1) Seeed Studio 313070004 (Seeed Studio, 2025); and (2) OSEPP SC10036 (OSEPP, 2025).

4.1. I-V and P-V results

As an example, the I-V and P-V curves for 95 °C and 75 °C are depicted in Figs. 3 to 6, for the OSEPP SC10036 modules.

With these results, the open-circuit voltage and maximum power present a high degradation while the short-circuit current also present a moderate degradation.

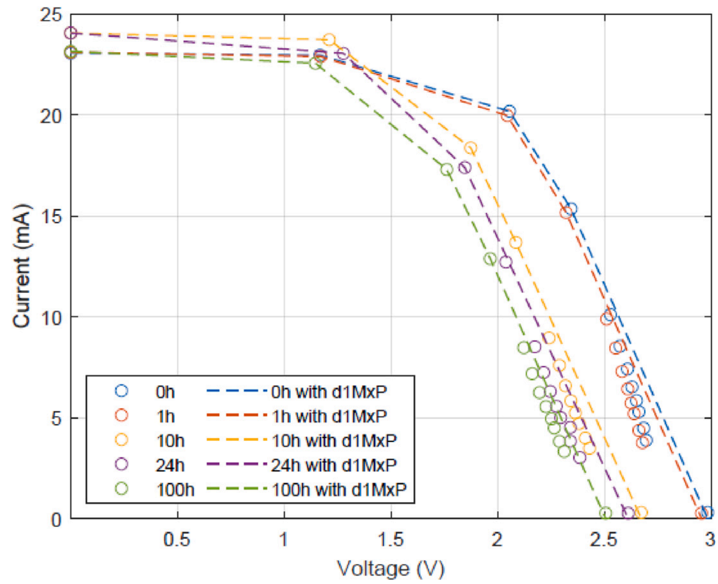

Fig. 5. Current–voltage curves of OSEPP SC10036 modules for 75 °C.

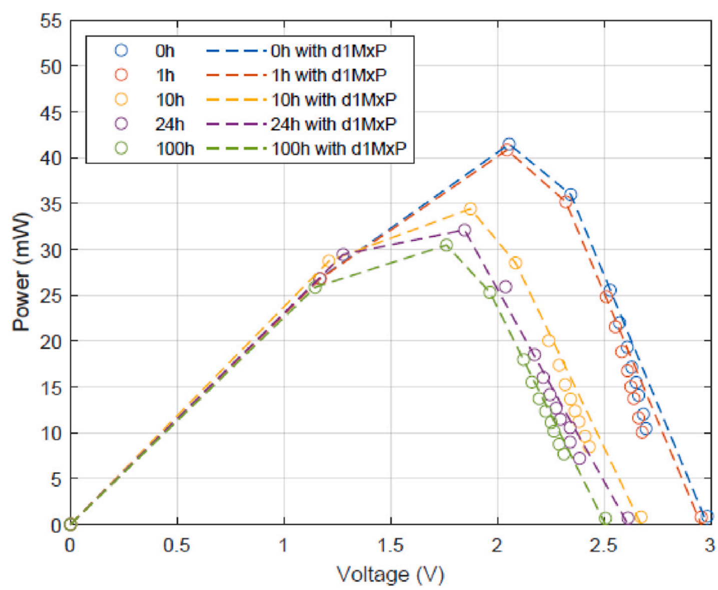

Fig. 6. Power-voltage curves of OSEPP SC10036 modules for 75 °C.

Figs. 7 and 8 contain all the linear regressions for all the tested temperatures over the test time, for the two variables under study on the Seeed Studio 179–3740 modules, V_{oc} and P_{max}, respectively. The same for the OSEPP SC10036 modules in Figs. 9 and 10.

It was found that both V_{oc} and P_{max} depends logarithmically on time, as modelled by expression set (5). An important note should be highlighted: this is not the Arrhenius Model. Although both are logarithm variations, this represent the ageing over time, whereas from the Arrhenius Model one presents the time for a certain parameter decrease as a function of test temperature.

$$\begin{cases} V_{oc}(t) = C_s ln(t) + C_y \\ P_{max}(t) = C_s ln(t) + C_y \end{cases} \tag{5}$$

C_s and C_y are respectively the slope and y-intercept value coefficients of the $ln(t)$ linear regression, in which t is the test time. This expression set is useful to estimate the time required for the module to present a determined percentage of loss for each parameter (open-circuit voltage and maximum power). Then, by repeating this process for all ageing temperatures, the Arrhenius model can be applied to estimate the required time to age under normal conditions. They are presented in Tables 1 and 2, respectively for the Seeed Studio 179–3740 modules as well as in Tables 3 and 4 for the OSEPP SC10036 modules. In these tables are also the coefficient of determination, R^2. They take values very close to 1 for almost every temperature, confirming that the linear regression fits very well the results of the tests.

As expected, the cells under study experience the typical decrease in open circuit voltage and maximum power, with the increase in oven test temperature.

Also, it can be seen that, as the temperature rises, the logarithmic regression that defines the evolution of V_{oc} and P_{max} as a higher slope.

4.2. Arrhenius model

The Arrhenius model is applied to the experimental results obtained in Section 4.1. The results are shown in Figs. 11 and 12, respectively for the Seeed Studio 179–3740 and the OSEPP SC10036 modules. The

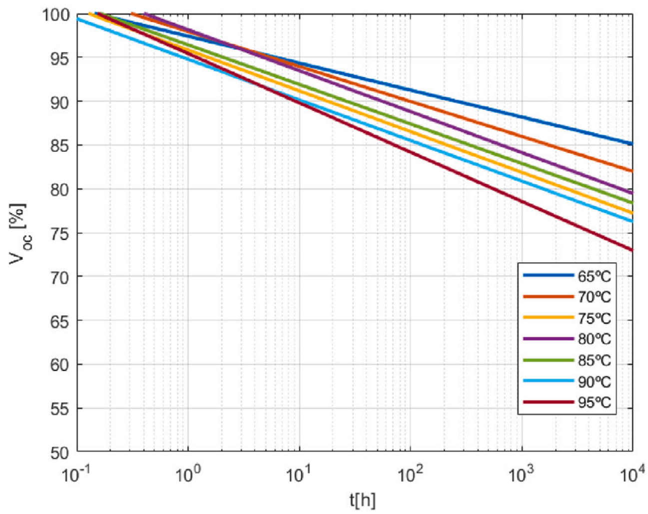

Fig. 7. V_{oc} over test time for the Seeed Studio 179–3740 modules.

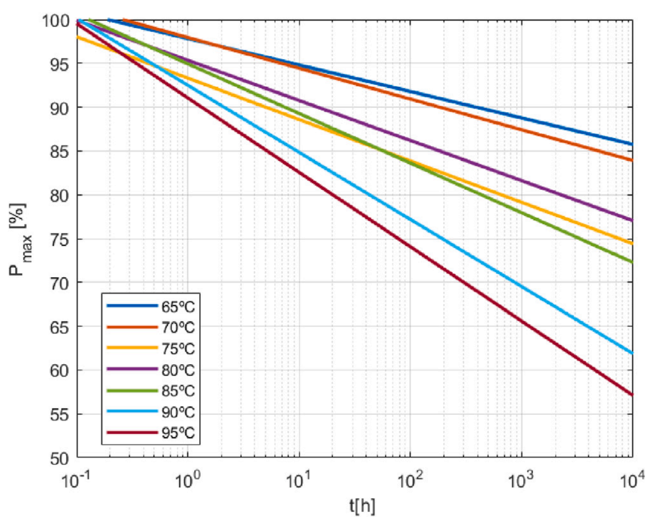

Fig. 8. P_{max} over test time for the Seeed Studio 179–3740 modules.

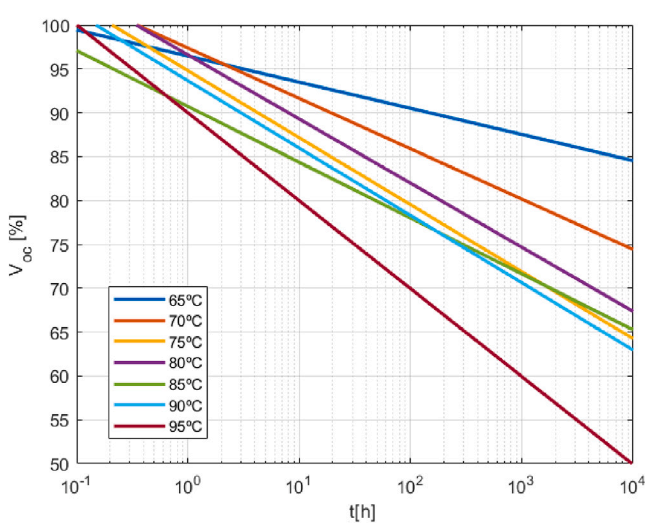

Fig. 9. V_{oc} over test time for the OSEPP SC10036 modules.

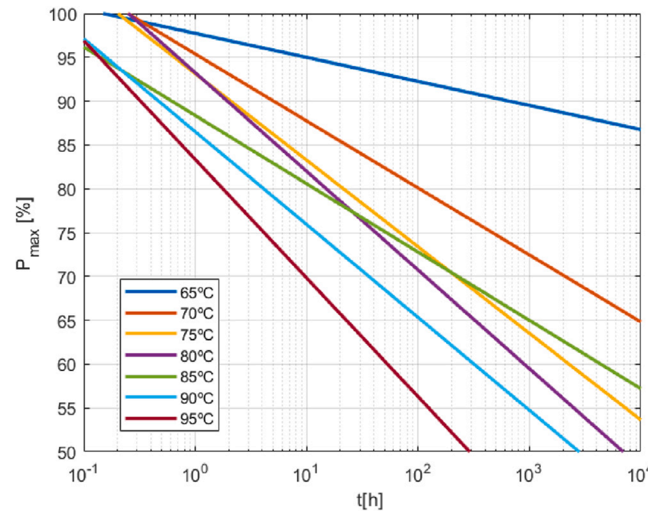

Fig. 10. P_{max} over test time for the OSEPP SC10036 modules.

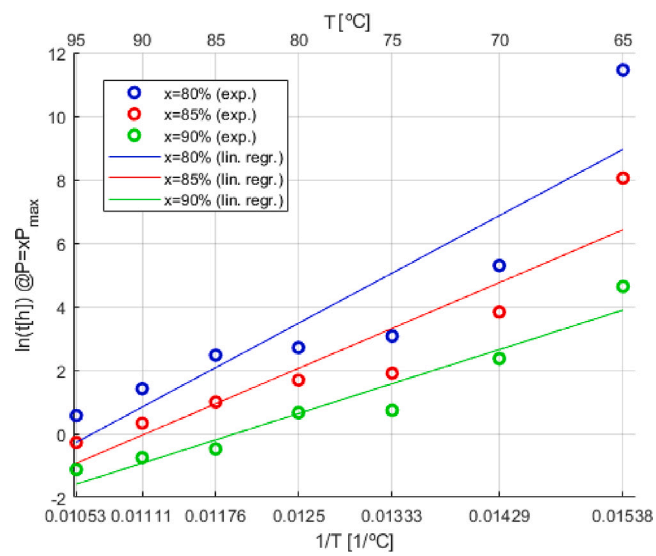

Fig. 11. Arrhenius plots of the power degradation over test time for the Seeed Studio 179–3740 modules.

Table 1
Coefficients of the linear regression of V_{oc} for each temperature tested, for the Seeed Studio 179–3740 modules.

T (°C)	C_s	C_y	R^2
65	−1.337	97.417	0.970
70	−1.734	97.951	0.774
75	−2.022	95.838	0.985
80	−2.029	98.149	0.673
85	−1.960	96.425	0.896
90	−2.012	94.777	0.987
95	−2.442	95.430	0.927

dots represent the experimental points and the lines the Arrhenius plots for a maximum power decrease of 10%, 15% and 20%.

With these data and assuming a normal operation under an average of 45 °C (given by Nominal Operating Cell Temperature — NOCT), one can estimate how much time it takes for the module to lose a certain percentage of its maximum power. This is done using expression (4), extrapolating the time (yy-axis in Arrhenius plots) for which the temperature (xx-axis in Arrhenius plots) is, in this case, 45 °C.

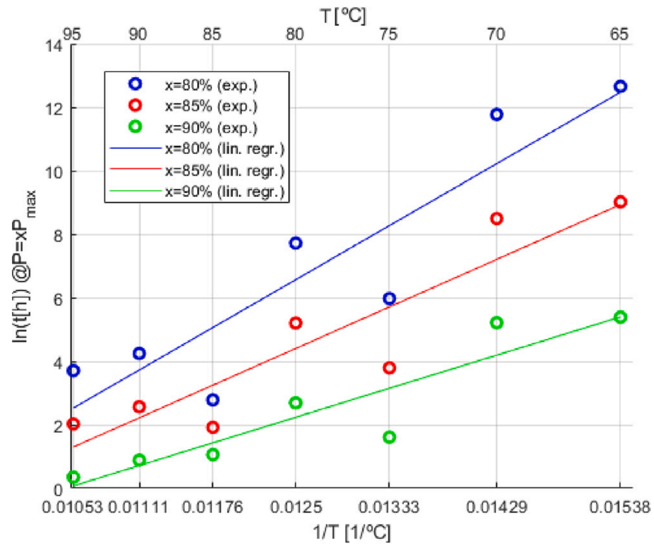

Fig. 12. Arrhenius plots of the power degradation over test time for the OSEPP SC10036 modules.

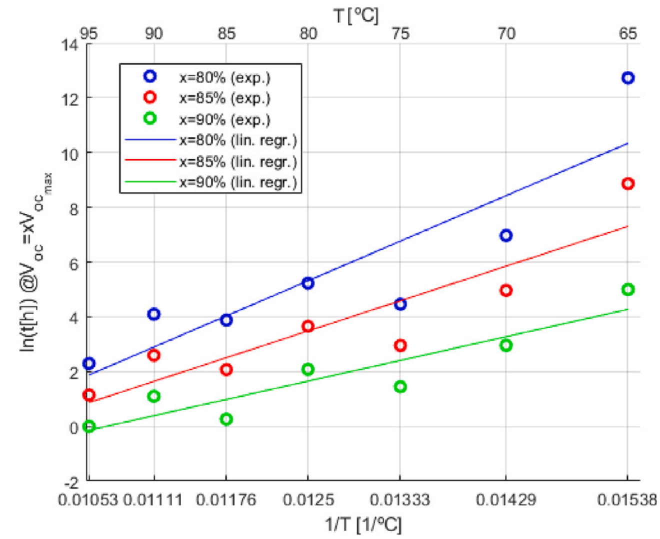

Fig. 13. Arrhenius plots of the open circuit voltage degradation over test time for the Seeed Studio 179–3740 modules.

Table 2
Coefficients of the linear regression of P_{max} for each temperature tested, for the Seeed Studio 179–3740 modules.

T (°C)	C_s	C_y	R^2
65	−1.312	97.826	0.823
70	−1.525	97.949	0.739
75	−2.053	93.311	0.754
80	−1.988	95.342	0.976
85	−2.461	94.940	0.830
90	−3.326	92.490	0.962
95	−3.687	91.045	0.743

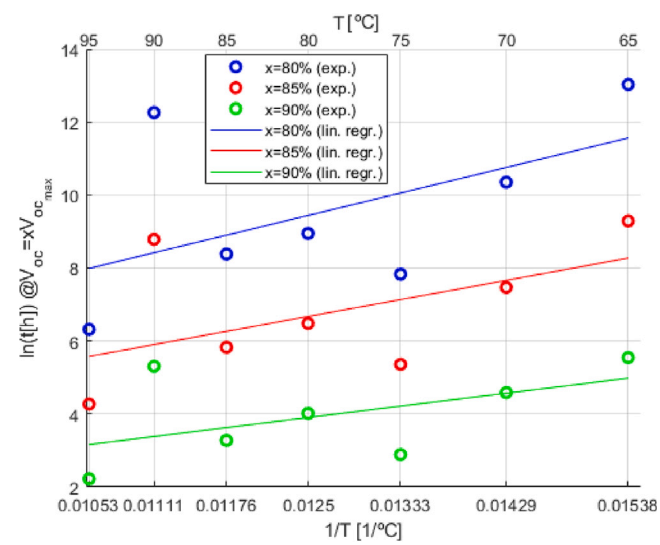

Fig. 14. Arrhenius plots of the open circuit voltage degradation over test time for the OSEPP SC10036 modules.

Table 3
Coefficients of the linear regression of V_{oc} for each temperature tested, for the OSEPP SC10036 modules.

T (°C)	C_s	C_y	R^2
65	−1.294	96.469	0.964
70	−2.494	97.383	0.732
75	−3.318	94.801	0.926
80	−3.176	96.606	0.651
85	−2.765	90.725	0.870
90	−3.335	93.655	0.919
95	−4.354	89.999	0.935

Table 4
Coefficients of the linear regression of P_{max} for each temperature tested, for the OSEPP SC10036 modules.

T (°C)	C_s	C_y	R^2
65	−1.191	97.738	0.903
70	−3.319	95.384	0.709
75	−4.290	93.144	0.929
80	−4.889	93.251	0.856
85	−3.384	88.368	0.870
90	−4.601	86.517	0.690
95	−5.878	83.356	0.902

Based on these results, it is concluded that the Seeed Studio 179–3740 modules lose 10% of their maximum power in 12 years and 5 months, whereas the OSEPP SC10036 modules lose it in 45 years and 1 month. Although both solar cells are from the same technology (monocrystalline silicon solar cells), they are from different manufactures, and consequently, the fabrication processes are distinct. This justifies the results divergence and shows the necessity of analysing the device's performance for long periods instead of testing just for the present behaviour.

However, loss of power is not always the main problem. Often the modules are connected in strings to inverters or converters. For the system to work properly, it is necessary to guarantee minimum and maximum operating power limits for the string, as well as voltage limits. Thus, one should also analyse how ageing affects voltage for the same load, for instance, by analysing open-circuit voltage. These results are shown in Figs. 13 and 14, respectively for the Seeed Studio 179–3740 and the OSEPP SC10036 modules. The dots represent the experimental points and the lines the Arrhenius plots for a V_{oc} decrease of 10%, 15% and 20%.

As done for the maximum power, the loss of 10% in V_{oc} is forecast for 4 years and 1 month for the Seeed Studio 179–3740 module whereas the OSEPP SC10036 modules it takes 2 months.

Table 5
Data and time extrapolation of the Arrhenius model.

Module	Seeed Studio 179–3740		OSEPP SC10036	
Characteristic	P_{max}	V_{oc}	P_{max}	V_{oc}
E_a/k	1128.01	908.78	1095.72	373.610
$ln(A)$	−13.465	−9.707	−11.462	−0.767
R^2	0.94	0.85	0.85	0.30
Time to lose 10%	12y 5m	4y 1m	45y 1m	2m

5. Discussion

Table 5 details the model parameters and their time extrapolation for 10% power and voltage losses, considering expression (3). The results of the Arrhenius model for the P_{max} show a clear logarithmic dependence of this parameter with the temperature, as the Arrhenius model states, since the coefficient of determination, R^2, has a value very close to 1. The same logarithmic behaviour happens with the plots of V_{oc} of the Seeed device. Using this fit, the open-circuit voltage decays 10% in just 4 years and 1 month. The exception is the open-circuit voltage of the OSEPP module whose variation as almost no trend. The conclusion, also based on the coefficient of determination, is that the experimental points obtained do not follow Arrhenius model and consequently ageing should be determined. This would be overcome by adding lower temperatures points. However, it would increase drastically the real testing time which made it impossible to perform the experimental procedures.

Nonetheless, both modules' maximum power loss times are within the expected in literature (Jordan and Kurtz, 2013; Sreejith et al., 2022; Doumane et al., 2015a; Gyamfi et al., 2023; Doumane et al., 2015b; Otth and Ross, 1983). The average degradation rate of the maximum power of these cells is 0.80% and 0.22% per year, for the Seeed and OSEPP modules, respectively. Nonetheless, the results of both models suggest that the modules characteristics would decay between 10% and 15% in 25 years, which is the standard commercial warranties.

6. Conclusion

In this research work, modules from two different manufacturers are under accelerated ageing tests and their operation is analysed at different times, establishing their lifetimes.

Modules are aged in constant temperature experiments but repeated for different temperatures following the hypothesis underlined by the Arrhenius model. The results showed a constant decrease in the output power and in the open circuit voltage with the test time, as anticipated.

The behaviour of both P_{max} was successfully modelled using a logarithmic regression over time, which showed a strong fit with experimental data.

The Arrhenius model applied to P_{max} showed a clear logarithmic dependence on temperature. The analysis indicated that the solar cells used in the tests would lose approximately 10% of their maximum power output between 12 and 45 years, depending on the manufacturer, a time frame longer than the usual warranty of a PV solar cell. The V_{oc} revealed a much faster degradation rate, with a voltage decrease of 10% in approximately 4 years, for the cells' whose performance followed the logarithm behaviour.

Comparing the cells from different manufacturers, one can conclude that the degradation rates and the stability of the cells differ from manufacturer to manufacturer. The two different models of solar cells studied showed a maximum power degradation ranging of 0.80% and 0.22% per year, depending not only on the device technology but also on its fabrication processes. This fact leads one to conclude that the reliability of some solar cells that are available in the market cannot be assured. The results of the tests performed were plausible and followed what can be found in the literature (Gebhardt et al., 2025; Doumane et al., 2015a; Gyamfi et al., 2023; Doumane et al., 2015b; Otth and Ross, 1983; Jordan and Kurtz, 2013; Sreejith et al., 2022).

Within the 25-year commercial warranties the results also suggest that both power and voltage characteristics will decay between 10% to 15% (Doumane et al., 2015a; Jordan and Kurtz, 2013). By providing data on how solar cells from various manufacturers perform, this study lays the groundwork for improving the quality and reliability of solar cells.

In conclusion, this study successfully characterises the ageing process of photovoltaic solar cells. As photovoltaic solar energy becomes a cornerstone of the global shift towards renewable energy, the performance and stability under the ageing of photovoltaic solar cells are more important than ever.

CRediT authorship contribution statement

Rui G. Marques Araújo: Writing – original draft, Software, Methodology, Investigation, Formal analysis, Conceptualization. **Ricardo A. Marques Lameirinhas:** Writing – review & editing, Writing – original draft, Visualization, Validation, Supervision, Software, Resources, Methodology, Investigation, Funding acquisition, Formal analysis, Conceptualization. **João Filipe Pereira Fernandes:** Writing – review & editing, Visualization, Validation, Supervision, Software, Resources, Methodology, Investigation, Formal analysis, Data curation, Conceptualization. **Rui J. Tomás Oliveira:** Writing – review & editing, Investigation. **Catarina P. Correia V. Bernardo:** Visualization, Investigation. **João Paulo N. Torres:** Visualization, Project administration, Funding acquisition.

Declaration of competing interest

The authors declare that they have no known competing financial interests or personal relationships that could have appeared to influence the work reported in this paper.

Acknowledgements

This work was supported by FCT - Fundação para a Ciência e Tecnologia, I.P. by project reference UIDB/50008: Instituto de Telecomunicações.

The authors also acknowledge Fundação para a Ciência e Tecnologia (FCT) for its financial support via the projects LAETA Base Funding (DOI: 10.54499/UIDB/50022/2020) and LAETA Programatic Funding (DOI: 10.54499/UIDP/50022/2020).

Data availability

Data will be made available on request.

References

Adak, S., Cangi, H., Yilmaz, A.S., Arifoglu, U., 2023. Development software program for extraction of photovoltaic cell equivalent circuit model parameters based on the Newton–Raphson method. J. Comput. Electron. http://dx.doi.org/10.1007/s10825-022-01969-8.

Barbato, M., Barbato, A., Meneghini, M., Tavernaro, G., Rossetto, M., Meneghesso, G., 2017. Potential induced degradation of N-type bifacial silicon solar cells: An investigation based on electrical and optical measurements. Sol. Energy Mater. Sol. Cells 168, 51–61. http://dx.doi.org/10.1016/j.solmat.2017.04.007.

Bernardo, Catarina P Correia V, Lameirinhas, Ricardo A Marques, Martins, Sofia Lima, Torres, João Paulo N, Baptista, António, Martins, Maria João M, Santos, Marcelino, 2024. Experimental investigation and modelling of the temperature effect in mono-si solar cells using the novel d1MxP model. In: 2024 IEEE 22nd Mediterranean Electrotechnical Conference. MELECON, IEEE, pp. 86–91, URL: https://www.doi.org/10.1109/MELECON56669.2024.10608722.

Doumane, R., Balistrou, M., Logerais, P.O., Riou, O., Durastanti, J.F., Charki, A., 2015a. A Circuit-Based Approach to Simulate the Characteristics of a Silicon Photovoltaic Module With Aging. J. Sol. Energy Eng. 137 (2), 021020, URL: https://www.doi.org/10.1115/1.4029541.

Doumane, R., Balistrou, M., Logerais, P.O., Riou, O., Durastanti, J.F., Charki, A., 2015b. A Circuit-Based Approach to Simulate the Characteristics of a Silicon Photovoltaic Module With Aging. J. Sol. Energy Eng. 137 (2), 021020. http://dx.doi.org/10.1115/1.4029541.

El Chaar, L., lamont, L.A., El Zein, N., 2011. Review of photovoltaic technologies. Renew. Sustain. Energy Rev. 15 (5), 2165–2175. http://dx.doi.org/10.1016/j.rser.2011.01.004.

Gebhardt, Paul, Marletti, Simone, Markert, Jochen, Kräling, Ulli, Tu, Mai, Haedrich, Ingrid, Philipp, Daniel, 2025. Comparison of commercial topcon PV modules in accelerated aging tests. IEEE J. Photovolt. 15 (1), 24–29, URL: https://www.doi.org/10.1109/JPHOTOV.2024.3483317.

Gul, Mehreen, Kotak, Yash, Muneer, Tariq, 2016. Review on recent trend of solar photovoltaic technology. Energy Explor. Exploit. 34 (4), 485–526. http://dx.doi.org/10.1177/0144598716650552.

Gyamfi, Samuel, Aboagye, Bernard, Peprah, Forson, Obeng, Michael, 2023. Degradation analysis of polycrystalline silicon modules from different manufacturers under the same climatic conditions. Energy Convers. Manag.: X 20, 100403, URL: https://doi.org/10.1016/j.ecmx.2023.100403.

Jordan, D., Kurtz, Sarah, 2013. Photovoltaic degradation rates—an analytical review. Prog. Photovolt., Res. Appl. 21, URL: https://www.doi.org/10.1002/pip.1182.

Jordan, Dirk C., Kurtz, Sarah R., VanSant, Kaitlyn, Newmiller, Jeff, 2016. Compendium of photovoltaic degradation rates. Prog. Photovolt., Res. Appl. 24 (7), 978–989, URL: https://www.doi.org/10.1002/pip.2744.

King, D.L., Kratochvil, J.A., Boyson, W.E., 2000. Stabilization and performance characteristics of commercial amorphous-silicon PV modules. In: Conference Record of the Twenty-Eighth IEEE Photovoltaic Specialists Conference - 2000 (Cat. No.00CH37036). pp. 1446–1449. http://dx.doi.org/10.1109/PVSC.2000.916165.

van Leest, Rosalinda H., Mulder, Peter, Gruginskie, Natasha, van Laar, Simone C.W., Bauhuis, Gerard J., Cheun, Hyenseok, Lee, Heonmin, Yoon, Wonki, van der Heijden, Remco, Bongers, Ed, Vlieg, Elias, Schermer, John J., 2017. Temperature-induced degradation of thin-film III–V Solar cells for space applications. IEEE J. Photovolt. 7 (2), 702–708, URL: https://www.doi.org/10.1109/JPHOTOV.2016.2642642.

Libby, Cara, Paudyal, Bijaya, Chen, Xin, Hobbs, William B., Fregosi, Daniel, Jain, Anubhav, 2023. Analysis of PV module power loss and cell crack effects due to accelerated aging tests and field exposure. IEEE J. Photovolt. 13 (1), 165–173, URL: https://www.doi.org/10.1109/JPHOTOV.2022.3228104.

Marques Lameirinhas, Ricardo A., Torres, João Paulo N., de Melo Cunha, João P., 2022. A photovoltaic technology review: History, fundamentals and applications. Energies 15 (5), URL: https://www.doi.org/10.3390/en15051823.

Mughal, Shafqat, Sood, Yog, Jarial, R., 2018. A review on solar photovoltaic technology and future trends.

OSEPP, 2025. OSEPP 10036. URL: https://osepp.com/accessories/solar-cells.

Ott, Thomas, Walter, Thomas, Hariskos, Dimitrios, Kiowski, Oliver, Schäffler, Raymund, 2013. Accelerated aging and contact degradation of CIGS solar cells. IEEE J. Photovolt. 3 (1), 514–519, URL: https://www.doi.org/10.1109/JPHOTOV.2012.2226141.

Otth, D.H., Ross, Ronald G., 1983. Assessing photovoltaic module degradation and lifetime from long term environmental tests. URL: https://api.semanticscholar.org/CorpusID:109244682. (Accessed December 2023).

Rathore, Neelam, Panwar, Narayan Lal, Yettou, Fatiha, Gama, Amor, 2021. A comprehensive review of different types of solar photovoltaic cells and their applications. Int. J. Ambient Energy 42 (10), 1200–1217. http://dx.doi.org/10.1080/01430750.2019.1592774.

Seeed Studio, 2025. Seeed studio 313070004. URL: https://www.seeedstudio.com/0-5W-Solar-Panel-55x70.html?srsltid=AfmBOorvdUzvs3Ym3pn7ObT98d8UswdxoKWjdbMXdskrihl0kjoReA83.

Shin, Sooeun, Shin, Hyunjung, 2023. Aging of perovskite solar cells: a mini review. Mater. Today Energy 37, 101381. http://dx.doi.org/10.1016/j.mtener.2023.101381.

Sinha, Archana, Gopalakrishna, Hamsini, Bala Subramaniyan, Arun, Jain, Deepak, Oh, Jaewon, Jordan, Dirk, TamizhMani, GovindaSamy, 2020. Prediction of climate-specific degradation rate for photovoltaic encapsulant discoloration. IEEE J. Photovolt. 10 (4), 1093–1101, URL: https://www.doi.org/10.1109/JPHOTOV.2020.2989182.

Sreejith, S., Ajayan, J., Reddy, Kollem Sreedhar, Sivasankari, B., 2022. A comprehensive review on thin film amorphous silicon solar cells. Silicon 14, URL: https://www.doi.org/10.1007/s12633-021-01644-w.

Torres, João Paulo, Lameirinhas, Ricardo, Pinho Correia Valério Bernardo, Catarina, Martins, Sofia, Santos, P. Mendonça dos, Veiga, H., Martins, Maria, Figueiredo, Paula, 2023a. Analysis of different third-generation solar cells using the discrete electrical model d1MxP. Energies 16, 3289, URL: https://www.doi.org/10.3390/en16073289.

Torres, João Paulo N, Marques Lameirinhas, Ricardo A, Correia V. Bernardo, Catarina P, Veiga, Helena Isabel, dos Santos, Pedro Mendonça, 2023b. A discrete electrical model for photovoltaic solar cells—d1MxP. Energies 16 (4), 2018.

Tyan, Yuan-Sheng, 1988. Topics on thin film CdS/CdTe solar cells. Sol. Cells 23 (1), 19–29, Special Issue on Cadmium Telluride.

Zhou, Jing, Liu, Zonghao, Yu, Peng, Tong, Guoqing, Chen, Ruijun, Ono, Luis K., Chen, Rui, Wang, Haixin, Ren, Fumeng, Liu, Sanwan, Wang, Jianan, Lan, Zhigao, Qi, Yabing, Chen, Wei, 2023. Modulation of perovskite degradation with multiple-barrier for light-heat stable perovskite solar cells. Nat. Commun. 14, URL: https://www.doi.org/10.1038/s41467-023-41856-9.